

CHAPTER 2

Materials and methods

2.1 Phytochemical Structures for P-gp inhibitors

For library generation regarding the groups of phytochemicals used as compound sets, herbal compounds with experimental induced/inhibitory activities were taken from a variety of publications based on structural diversity and activity covering. Selected phytochemicals were from various frequently used Thai medicinal plants and may be well known for many years of clinical applications such as CAM and/or Thai traditional medicines, or used as commercial dietary/herbal supplements. They were classified into the same phytochemical group.

The most herbal constituents in Thai medicinal plants are phenolic compounds especially flavonoids. Moreover, flavonoids are major plant secondary metabolites and represent the most studied phytochemicals (Boonsong et al., 2011). Thus this class of herbal compounds with known P-gp inhibitory activity was utilised as a template (training set) for model creation to elucidate the inhibition of Thai herbal ingredients to P-gp and an external test set for a validation test of the created model in this QSAR study, and also used in the molecular docking and dynamics simulation studies.

2.2 QSAR modelling for P-gp inhibitors

Herbal compounds were chosen as a training set on the basis of ensuing criteria to generate a fine QSAR model: by engulfing an extensive activity range of chemicals that comprise the most active, moderate, and less active or inactive inhibitors, and including inducers (Shukla et al., 2014). Flavonoids with P-gp induced/inhibitory studies were identified from various publications. These substances are natural compounds with the known activity for P-gp inhibition. The number of compounds/phytochemicals in each training set should be at least twenty, and approximate ten compounds/phytochemicals should be in each of the test or external

evaluation sets (Davis & Vasanthi, 2015). The number of predictor variables (descriptors) defines the training set size. It is ordinarily accepted that there must be at least five compounds for one descriptor (Topliss ratio) for a facile method as multiple linear regression (MLR) (Kiralj & Ferreira, 2009).

The 23 flavonoids and their induced/inhibitory activities were obtained from two publications (Gyémant et al., 2005; Martins et al., 2010). The bioassay (fluorescence activity ratio; FAR at 40 $\mu\text{g/ml}$ which represents P-gp induction or inhibition) values of the 23 flavonoids cover the range from 0.5–46.4. From the preliminary study using bioassay (FAR) as a dependent variable, the obtained correlation was low and increased higher in models with excessive descriptors. The FAR values were transformed becoming the corresponding pFAR ($-\log \text{ FAR}$) values, which is in the range of -1.67–0.3. The use of pFAR is to represent a negative value (-) as a P-gp inhibitory activity and a positive value (+) as a P-gp induced activity. Flavonoids with FAR values >1 but <10 ($\text{pFAR} < 0$ but > -1) were regarded to be active inhibitors (weak inhibitors) of P-gp and flavonoids with FAR values >10 ($\text{pFAR} < -1$) were considered as potent (or strong) inhibitors (Sousa, Ferreira, Molnár, & Fernandes, 2013). A list of the flavonoid molecular structures are illustrated in Table 2.1 and further details on their corresponding experimental FAR and pFAR values (Gyémant et al., 2005; Martins et al., 2010) are illustrated in Table 2.1.

ลิขสิทธิ์มหาวิทยาลัยเชียงใหม่
Copyright© by Chiang Mai University
All rights reserved

Table 2.1 Molecular structures of bioflavonoids with FAR values (in the parenthesis) of the training set. 1-21 are from Gyémant et al. (Gyémant et al., 2005), and 22-23 are from Martins et al. (Martins et al., 2010)

1. Formononetin (18.3)	2. Amorphigenin (46.4)	3. Afrormosin (3.1)
4. 6a,12a-Dehydroamorphigenin (3.0)	5. (+)-12-Hydroxyamorphigenin (Dabinol) (2.8)	6. Rotenone (28.6)
7. Catechin (2.9)	8. Neohesperidin (2.8)	9. Naringin (2.3)
10. Chrysin (14.6)	11. Robinin (1.5)	12. Floretin (Phloretin) (4.9)

Table 2.1 (continued)

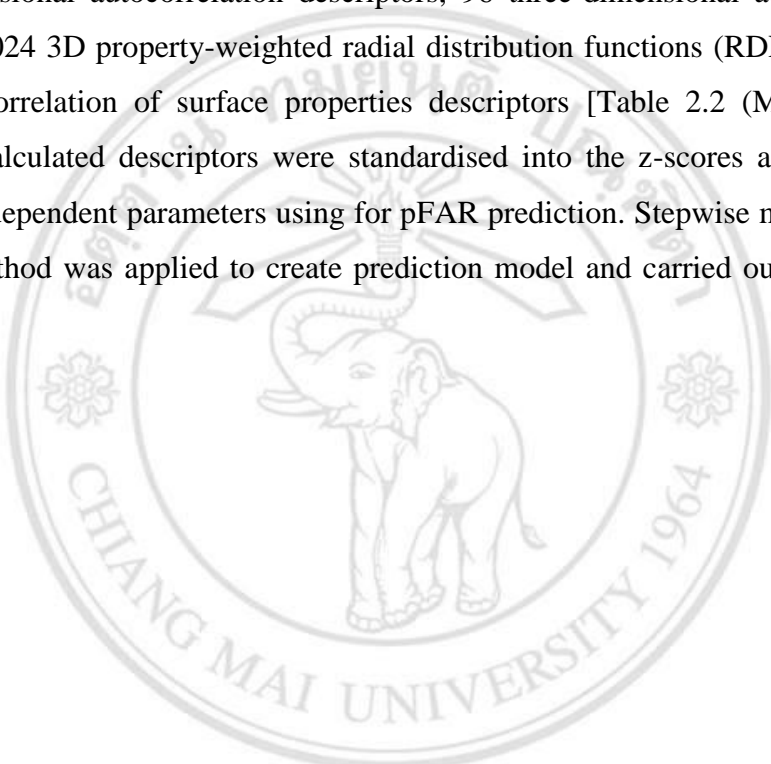
13. Floridzin (Phlorhizin) (0.6)	14. Robinetin (0.7)	15. Dihydrorobinetin (0.7)
16. Kaempferol (0.8)	17. Dihydrofisetin (fustin) (0.5)	18. Dihydroquercetin (0.6)
19. Sakuranin (0.8)	20. Sakuranetin (2.4)	21. Epigallocatechin (36.1)
22. Epicatechin (0.97)	23. Procyanidin B5 (0.58)	

2.2.1 Preparing of molecular structures

The all the two-dimensional (2D) structures of flavonoids were sketched using the ChemBioDraw Ultra. And then, the 2D structures were transformed into three-dimensional (3D) structures by using the ChemBio3D Ultra. Every hydrogen atom is regarded during the computing process for each molecule. Energy minimisation and optimisation of molecular 3D structure were also carried out utilising the ChemBio3D Ultra by MM2 forcefield.

2.2.2 Generation of molecular descriptors

The ADRIANA.Code programme (Version 2.0) was employed to compute physicochemical parameters of the molecular structures of flavonoids. This programme consists unique combining procedures for computing molecular structure descriptors on a physicochemical basis and sound geometric. A total of 1252 descriptors were computed utilising this programme including 8 global molecular descriptors, 88 two-dimensional autocorrelation descriptors, 96 three-dimensional autocorrelation descriptors, 1024 3D property-weighted radial distribution functions (RDF) descriptors and 36 autocorrelation of surface properties descriptors [Table 2.2 (Mueller et al., 2010)]. All calculated descriptors were standardised into the z-scores and then were selected as independent parameters using for pFAR prediction. Stepwise multiple linear regression method was applied to create prediction model and carried out using SPSS Statistics 17.0.



ลิขสิทธิ์มหาวิทยาลัยเชียงใหม่
Copyright© by Chiang Mai University
All rights reserved

Table 2.2 Summary of 35 categories comprising 1252 molecular descriptors calculated using ADRIANA.Code

	description method	description property	abbreviation	number
1	scalar descriptors	molecular weight of compound	Weight	1
2		number of hydrogen bonding acceptors	HDon	1
3		number of hydrogen bonding donors	HAcc	1
4		octanol/water partition coefficient in [log units]	XlogP	1
5		topological polar surface area in [Å ²]	TPSA	1
6		mean molecular polarizability in [Å ³]	Polariz	1
7		dipole moment in [Debye]	Dipol	1
8		solubility of the molecule in water in [log units]	LogS	1
9	2D autocorrelation	atom identities	2DA_Ident	11
10		σ atom charges	2DA_SigChg	11
11		π atom charges	2DA_PiChg	11
12		total charges	2DA_TotChg	11
13		σ atom electronegativities	2DA_SigEN	11
14		π atom electronegativities	2DA_PiEN	11
15		lone pair electronegativities	2DA_LpEN	11
16		effective atom polarizabilities	2DA_Polariz	11
17	3D autocorrelation	atom identities	3DA_Ident	12
18		σ atom charges	3DA_SigChg	12
19		π atom charges	3DA_PiChg	12
20		total charges	3DA_TotChg	12
21		σ atom electronegativities	3DA_SigEN	12
22		π atom electronegativities	3DA_PiEN	12
23		lone pair electronegativities	3DA_LpEN	12
24		effective atom polarizabilities	3DA_Polariz	12
25	radial distribution function	atom identities	RDF_Ident	128
26		σ atom charges	RDF_SigChg	128
27		π atom charges	RDF_PiChg	128
28		total charges	RDF_TotChg	128
29		σ atom electronegativities	RDF_SigEN	128
30		π atom electronegativities	RDF_PiEN	128
31		lone pair electronegativities	RDF_LpEN	128
32		effective atom polarizabilities	RDF_Polariz	128
33	surface autocorrelation	molecular electrostatic potential	Surf_ESP	12
34		hydrogen bonding potential	Surf_HBP	12
35		hydrophobicity potential	Surf_HPP	12
	total			1252

2.2.3 Statistical methods for QSAR modelling

Quantitative structure-activity relationship analysis is a statistical method by which the molecular structures of compounds are correlated with a well-specified parameter quantitatively, like chemical reactivity or biological activity. For instance, pharmacological activity can be quantitated as in the concentration of a compound needed to provide an exact pharmacological response. In addition, when structures or physicochemical properties of molecules are quantitated to be numbers, one can produce an arithmetical relationship (QSAR), among the two. The arithmetical exposition can thereupon be applied to predict the pharmacological effect of other molecular structures. Most universal arithmetical function of QSAR is the following;

$$\text{Activity} = f(\text{physicochemical properties and/or structural properties})$$

An advancement of a quantitative structure-activity relationship model results in the endeavours to increasingly discover corresponding relationships among the variations in the values of molecular properties and the pharmacological effect for a chemical set/series which can thereupon be utilised to appraise activities of novel molecular identities (Yadav et al., 2010).

For identification of the predicted inhibitory activity of the untested phytochemicals, QSAR study is operated. A totality of physicochemical properties (descriptors) are utilised for the purpose of QSAR model creation. Physicochemical parameters of the herbal compound molecules are computationally calculated, then total of descriptors are obtained (used as an independent variable). Flavonoids were involved and P-gp inhibition was regarded as the biological activity parameter of the chemicals (a dependent variable). A statistical model was then utilised to predict the P-gp inhibitory activity of other flavonoids from herbs. A stepwise multiple linear regression method was used to establish a predictive model. Molecular descriptors for a QSAR model construction were selected (Yan et al., 2011). All calculated descriptors were selected as independent variables and P-gp inhibitory activity as dependent variables.

Based on the flavonoid compounds in dataset, all of these 23 compounds were used as the training set and their molecular descriptors [as standardised values (z-scores)] for the QSAR model construction were selected. Following the analysis method from the study of Yan et al. (Yan et al., 2011), Pearson's correlation coefficient (r) analysis merged with stepwise variable selecting manner was utilised to choose the best descriptor group for modelling. Regarding this study, molecular descriptors whose the calculated Pearson's correlation coefficient with the P-gp modulatory activity was less than 0.1 ($r < 0.1$) were not utilised.

After that by considering the pairwise correlation coefficients, if the pairwise correlation coefficient between any two descriptors was higher than 0.85, the descriptor, that had the lower correlation to the P-gp modulatory activity of a compound, one of them was eliminated. The remaining descriptors were selected utilising stepwise multiple linear regression (MLR) variable selecting method (Yan et al., 2011). First step, every descriptor chosen by correlation analysis were ranked in a descending sequence in accordance with their correlation coefficient with activity. Second step, the

descriptor which had the highest correlation coefficient with activity was utilised to create an ordinary linear regression model as an initial equation. Third step, other descriptors were subsequently admixed to the initial equation one by one. Subsequent admixing a new descriptor to the initial equation, a new equation was gained, and it was appraised with a significance test. If a significant accretion was accomplished, the admixed descriptor was kept, and if a significant accretion was not noticed, the admixed descriptor was eliminated. The procedure was reiterated till no descriptor could be admixed or eliminated (Zhong et al., 2013).

Many models were generated, but the best model satisfied all of the following parameters: (1) the number of compounds should be 3-6 times the number of molecular descriptors used in the proposed model (Agrawal et al., 2002), (2) R^2 , square of regression (>0.7) (Asgaonkar et al., 2013), (3) q^2 , cross-validated r^2 (>0.5) (Asgaonkar et al., 2013), (4) SEE, standard error of estimate (smaller is better) (Asgaonkar et al., 2013), (5) F-test, F-test for statistical significance of the model (higher is better, for the same set of descriptors and chemicals) (Asgaonkar et al., 2013).

To test the stability and predictive ability of the developed QSAR model, the model was validated utilising internal validation. The leave-one-out (q^2 , LOO) method was used to validate the model generated by MLR QSAR. Regarding the calculation of q^2 , each compound in the training set was sequentially moved away, the model was refit utilising same descriptors, and the pharmacological activity of the removed compound was predicted utilising the refit model. The q^2 was calculated utilising equation;

$$q^2 = 1 - \left[\frac{\sum (\hat{y}_i - y_i)^2}{\sum (y_i - y_{mean})^2} \right]$$

where y_i and \hat{y}_i are the actual and predicted activities of the i^{th} compound in the training set, respectively, and y_{mean} is the average activity of all compounds in the training set (Sharma et al., 2014).

2.2.4 Validation of a QSAR model

In order to evaluate the potential health risks related with herb-drug and/or food-drug interactions of some other flavonoids, the P-gp inhibitory activities of flavonoids in a dataset containing all 11 compounds (Table 3.3) was collected from recent literatures (Boccard et al., 2009; Chung et al., 2005; Kitagawa et al., 2004; Zhang & Morris, 2003) which were not included in the training set and estimated using the

developed QSAR model. The dataset were utilised like an external test set, which comprises all 11 active (weak) and strong inhibitors of P-gp. The values that stand for P-gp inhibitory activity of bioflavonoids from 4 literatures were converted into Inhibitory efficiency [calculated as percentage compared to a positive control (verapamil)]. The all the two-dimensional (2D) structures of 11 flavonoids were sketched using the ChemBioDraw Ultra. And then, the 2D structures were transformed into three-dimensional (3D) structures by using the ChemBio3D Ultra. All hydrogen atoms of each molecule are regarded during the computational process. Energy minimisation and optimisation of molecular 3D structure were also carried out utilising the ChemBio3D Ultra by MM2 forcefield. The ADRIANA.Code programme (Ver. 2.0) was applied to calculate physicochemical parameters of the 11 flavonoid molecules in the external test set.

All calculated descriptors were standardised into the z-scores and P-gp modulatory activity as pFAR values of each flavonoid were estimated using the MLR QSAR model.

2.3 Molecular docking of P-gp inhibitors

2.3.1 Preparing of P-gp protein

Molecular docking was carried out. The PDB file of the crystal structure of mouse P-glycoprotein; PDB code: 4Q9H (with the resolution of 3.40 Å). A sequence similarity search with the BLAST between mouse and human P-gps was run in the UniProt Knowledgebase (UniProtKB) (Magrane & Consortium, 2011). The sequence alignment obviously illustrated that whole parts of human and mouse P-gps shared high amino acid identity 87.3% and interestingly, the NBDs which are requisite to cleave ATP and to provide energy for the drug efflux process disclosed 100% amino acid identity (Saeed et al., 2015). Thus, this study has been performed molecular modellings applying a mouse P-gp that could be extrapolated the results directly to human. The macromolecule was exported to Discovery Studio Client 2.5 to be adjusted hydrogen atoms and minimised energies with the CHARMM forcefield. Then the P-gp was transformed to PDBQT format utilising AutoDockTools 1.5.6 and was set as the macromolecule NBD1 and NBD2 dockings were selected for molecular docking. The

experimental data regarding P-gp inhibitory activity of flavonoids was collected from the literatures (Table 3.4 and 3.9).

2.3.2 Collection and preparing of ligand molecules

AutoDock 4.2.6 was utilised to dock a set of 25 known bioflavonoids which exhibited experimental P-gp inhibitory activity (Table 3.4 and 3.9). The bioflavonoids and their P-gp inhibitory activities were obtained from previous publications; Gyémant et al., Martins et al., Chung et al., El-Readi et al., Kitagawa et al., and Zhang and Morris (Gyémant et al., 2005; Martins et al., 2010; Chung et al., 2005; El-Readi et al. 2010; Kitagawa et al., 2004; Zhang & Morris, 2003). The dataset was comprises all 8 strong and 17 active (weak) inhibitors of P-gp compared with verapamil (this cardiovascular drug acts as a strong P-gp inhibitor). The values that stand for P-gp inhibitory activity of bioflavonoids from all literatures were converted into percentage of inhibitory efficiency compared to a positive control (verapamil). A compound that exhibits same or more potency of verapamil was classified to be a strong or potent inhibitor of P-gp.

2D structures of the flavonoids were constructed using ChemBioDraw Ultra 11.0 and later converted to 3D structures utilising ChemBio3D Ultra 11.0. Every hydrogen atom is regarded during the computing process for each flavonoid molecule. Energy minimisation and optimisation of molecular 3D structures were also carried out utilising the ChemBio3D Ultra 11.0 by MM2 forcefield with default setup (minimum rms gradient of 0.010) until the minimum rms error became smaller than 0.100 kcal/mol Å. These molecules were then used as ligands for molecular docking. A grid box was apportioned to define docking spaces upon the NBDs of the macromolecule.

2.3.3 Docking method

The docking efforts were targeted the ATP binding sites to impede the ATP hydrolysis (by NBD1 and 2), that ATP is an energy source of the pump. NBDs are greatly conserved among ABC transporters, these pumps are definitely demanded like the mechanistic driving force for the operation of P-gp. Many previous researches have studied regarding inhibition of NBDs (Palmeira et al., 2012). A wide range of bioflavonoids (presumed to bind both NBDs) were used in our docking study for validations of the NBD1 and 2 models.

Flavonoids were docked into both NBDs of 4Q9H to determine their binding affinities represented by estimated free energy of binding values. Energies for each atom type in the ligand were calculated at each grid point utilising AutoGrid. The volume of the grid was set to mantle the cytosolic domain containing ATP-binding site on each NBD and vicinity with a grid-spacing interval of 0.375 Å with dimension $126 \times 126 \times 126$ Å. These calculated energies were afterwards employed to predict binding energies for each ligand. Molecular docking of flavonoids was carried out utilising AutoDock 4.2.6 via the Lamarckian algorithm due to its ordinary robustness (Badhan & Penny, 2006) and performed by default. Default docking parameters with 50 runs, a population size of 250, 2,500,000 evaluations, and 27,000 generations per tested ligand for each cycle were employed throughout the study. Ligand orientations were clustered into groups with a 1 Å cut-off. Docking poses of every ligand were retrieved from the correspondent dlg file and AutoDockTools 1.5.6 and PyMol were utilised for visual inspection of the molecular docking result and graphical representations of all poses. A final docked delegate of the potential binding mode of bioflavonoids was picked based on the selection of the compound having the lowest docked energy within the most populated cluster of the lowest possible energy (Badhan & Penny, 2006).

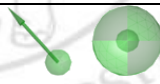
2.3.4 Validation of molecular docking

A correlation between a docking score (estimated free energy of binding) and an experimental activity (percentage of inhibitory efficiency) was performed. These values were plotted and the coefficient of determination (R^2) was admeasured. Experimentally admeasured activity values may correlate with calculated results, and increase and convince the reliability of related results when only computational results are available. (Palmeira et al., 2012) R^2 value must be obtained with a minimum of five points and higher than 0.6, a threshold routinely accepted to establish the goodness of structure-based models utilised in computational studies (Palmeira et al., 2012). Thus, afterwards the molecular docking calculation using AutoDock, the correlation between observed activities (percentage of inhibitory efficiency values) and computational docking scores (estimated free energies of binding), and including linear regression equation that can be further used to predict P-gp inhibitory activity of other flavonoids from inputted docking scores were determined.

2.3.5 NBD-based pharmacophore identification

The docked complexes of flavonoids at P-gp NBD1 and 2 were further examined using LigandScout software (Inte:Ligand version 3.12) (Wolber & Langer, 2004) to create schematic diagrams of protein–ligand interactions (binding modes). Pharmacophore models were created that pointed out certain amino acid residue atoms in NBDs interacted with the ligand atoms. The interactions created by LigandScout were presented as four main features, namely hydrogen bond donors (HBD), hydrogen bond acceptor (HBA), hydrophobic interactions (H) and aromatic ring (Ar). The feature shown in green colour is the HBD, red colour is HBA, yellow colour is H, and purple colour is Ar. Example representative pharmacophore features are shown in Table 2.3. Pharmacophore modelling for P-gp inhibitors was advocated by the availability of 3D structural data on protein–ligand complexes. Molecular interactions of the ligands to any binding cavities at NBDs were analysed in order to identify key features for ligand binding (Table 3.6 and 3.11). 4Q9H including ligands were overlaid to illustrate ligand binding cavities (Figure 3.2 and 3.4).

Table 2.3 Pharmacophore features from LigandScout

Chemical feature	Depiction style
HBD	
HBA	
H	
Ar	
Positive ionisable area	
Negative ionisable area	

2.4 Molecular dynamics (MD) simulations of P-gp inhibitors

2.4.1 Selection of a model and ligands for MD simulation

Five known flavonoids with strong experimental inhibitory activities of P-gp (Table 3.4 and 3.9); amorphigenin, epigallocatechin, rotenone, formononetin, and chrysin from the docking study were further used to realise the following: (1) dynamical effects of flavonoids on P-gp mediated efflux as competitive inhibitors, (2) dynamical

binding conformations and affinities of flavonoids that show strong P-gp inhibitory activities, (3) that NBD is the preferred binding site of flavonoids in a dynamical state, and (4) the physicochemical factors and interactions, which grant strong binding of flavonoids to P-gp in a dynamical state. These flavonoids have been proved to possess the strong inhibitory activity for P-gp (Gyémant et al., 2005). Therefore, they were used in the MD study to establish the computational techniques and elucidate that their observed P-gp inhibitory activities are on the basis of the competitive inhibition at ATP binding site within NBD2.

2.4.2 Preparing of P-gp–ligand complexes for MD simulation

3D models of protein–ligand complexes (at NBD2) obtained from molecular docking of 5 flavonoids; amorphenin, epigallocatechin, rotenone, formononetin, and chrysin to P-gp were analysed. The molecular docking provided illustration whether each flavonoid bound to NBD2 of P-gp or not (depended on a calculated binding affinity). Regarding MD simulation, stability of the molecular structures of each complex, calculation of binding free energy, hydrogen bond distance, and amino acid residue–ligand interaction energy decomposition were determined.

2.4.3 MD simulation method

All 5 docked complexes were conducted to molecular dynamics simulations. Every MD simulation was rendered utilising the AMBER 14 simulation package. The docked complexes was inserted into the dioleoyl-phosphatidylcholine (DOPC) bilayer modelled by the Lipid14 force field obtained from Dickson et al. (Dickson et al., 2014). The parameters for a ligand were generated by the Antechamber programme. The xleap module was run to prepare the complex prior to MD simulation. The standard AMBER force field (ff03.r1) was utilised to create the topologies and parameters of the complex (Palestro et al., 2014). Twelve Cl⁻ ions were put around the complex to keep the system's neutrality. The entire system was solvated in a truncated octahedral periodic box of TIP3P water molecules with a minimum solute-wall distance of 10 Å. All simulations were performed using PMEMD.CUDA from AMBER14 on graphics processing units (GPUs) GeForce GTX TITAN X manufactured by NVIDIA. Employing GPU would shorten the wall time of simulation desired to collect the

properties from each simulation (Götz et al., 2012; Le Grand et al., 2013; Salomon-Ferrer et al., 2013).

The MD simulations are operated utilising a time step of 2 femtoseconds. Potential energy for non-bonding interactions was calculated within the cut-off of 10 Å. The long range interactions were speculated utilising periodic boundary condition based on the Particle Mesh Ewald (PME) method. The SHAKE algorithm and the Langevin dynamics were employed to constrain a bond associating H atom, and handle the temperature, successively. Prior to MD simulations, the solvated systems were energy-minimised by a two-step minimisation procedure to eliminate possible bad contacts. First, the protein was fixed, and the water molecules were minimised by 8000 cycles of steepest descent and 4000 cycles of conjugate gradient minimisation by a force constant of 50 kcal/mol Å²; second, the whole system was minimised with no restraint by 2000 cycles (1500 cycles of steepest descent and 500 cycles of conjugate gradient minimisation). At first, the temperature of each system was increased gradually from 0 to 310 K over a period of 20 picoseconds (ps) of NVT dynamics. 60 ps of NVT equilibration was carried out. The equilibrated system was finally utilised for NPT production run for 15000 ps with 310 K and 1 atm pressure for properties collection. The coordinates of the P-gp–flavonoid complexes were saved every 1 ps. The VMD 1.9.2 (Humphrey et al., 1996) was utilised to visualise and analyse the simulation trajectory. The structural properties and intermolecular interactions of P-gp–flavonoid were analysed from the MD trajectories of 15 ns.

2.4.4 Dynamics conformational change analysis of the complexes

The dynamics conformational changes of the trajectory were checked by monitoring the equilibration of quantity; RMSD values of protein backbone (C_α, C, N) atoms throughout 15000 ps simulation with respect to the initial structure that the deviation of a target set of coordinates of each complex were measured using the CPPTRAJ utility in Amber Tools 15 (Roe & Cheatham, 2013).

2.4.5 Pre and post MD simulation binding mode comparison

Structure-based pharmacophore modelling provided illustration of molecular interaction features (binding modes) that amino acid residues essential for a binding of each flavonoid were clarified. Representative structures averaged over the 10000-15000

ps (trajectory stable stage) time frames were generated for the complexes using the CPPTRAJ utility so that the docked complexes of 5 flavonoids at 4Q9H NBD2 (representing pre MD simulation structures) including the generated average structures of the complexes (representing post MD simulation structures) at a stable stage were further examined using LigandScout (Wolber & Langer, 2004) to create 3D schematic diagrams of protein-ligand interactions (binding modes). 3D structure-based pharmacophore models were created that pointed out certain amino acid residue atoms in NBD2 interacted with ligand atoms. The interactions created by LigandScout were presented as four main features, namely hydrogen bond donors (HBD), hydrogen bond acceptor (HBA), hydrophobic interactions (H) and aromatic ring (Ar). The feature shown in green colour is the HBD, red colour is HBA, yellow colour is H, and purple colour is Ar. Molecular interactions of each ligand to any binding cavities at NBD2 were analysed in order to identify key features for ligand binding, as well as heavy atom distances representing hydrogen bonding interactions between each ligand and the protein were also measured using the CPPTRAJ utility (Figure 3.7-3.12).

2.4.6 Binding free energy calculation

The free energy of binding of each 4Q9H–flavonoid complex was computed relied on the Molecular Mechanics–Poisson-Boltzmann Surface Area (MM-PBSA) and Molecular Mechanic-Generalised Born Surface Area (MM-GBSA) protocols. The methodology details of both methods have been described elsewhere (Genheden & Ryde, 2015). Regarding this work, the free energy of binding of each trajectory was computed from the entire trajectory (1-15000 ps). The calculation was based on 150 snapshots from the respective trajectories.

The MM-PBSA and MM-GBSA analyses were implemented for each system depended on the MD trajectory, whereupon the free energy of binding is estimated perpetually:

$$\Delta G_{\text{bind}} = G_{\text{complex}} - (G_{\text{receptor}} + G_{\text{ligand}}) \quad (1)$$

$$\Delta G_{\text{bind}} = \Delta H - T\Delta S \approx \Delta E_{\text{MM}} + \Delta G_{\text{sol}} - T\Delta S \quad (2)$$

$$\Delta E_{\text{MM}} = \Delta E_{\text{internal}} + \Delta E_{\text{electrostatic}} + \Delta E_{\text{vdW}} \quad (3)$$

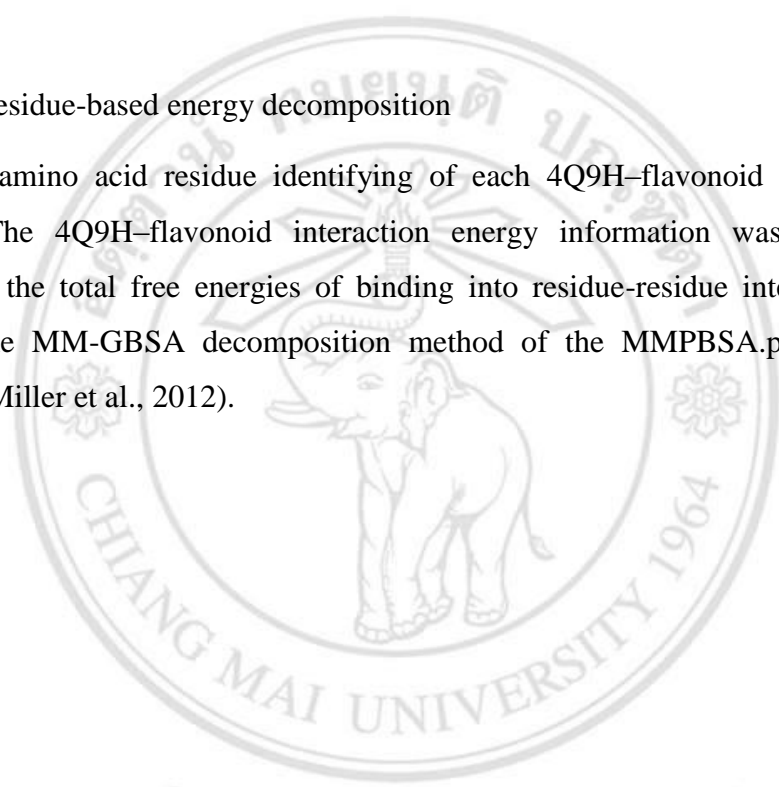
$$\Delta G_{\text{sol}} = \Delta G_{\text{PB/GB}} + \Delta G_{\text{SA}} \quad (4)$$

$$\Delta G_{\text{SA}} = \gamma\Delta A + b \quad (5)$$

where ΔG_{bind} points to the total free energy change between the bound-state (G_{complex}) and unbound-state systems ($G_{\text{receptor}} + G_{\text{ligand}}$), and can be decomposed into three terms: ΔE_{MM} , recognised as the gas-phase interaction energy, which comprises electrostatic ($\Delta E_{\text{electrostatic}}$) and van der Waals (ΔE_{vdW}) interactions; ΔG_{sol} , the solvation energy, which encloses the polar ($\Delta G_{\text{PB/GB}}$) and non-polar (ΔG_{SA}) components; and $-T\Delta S$, the change in the conformational entropy up to ligand binding, which was not respected in this work on account of the very high computational cost and low prediction accuracy (Sun et al., 2014).

2.4.7 Residue-based energy decomposition

A key amino acid residue identifying of each 4Q9H–flavonoid complex was performed. The 4Q9H–flavonoid interaction energy information was created via decomposing the total free energies of binding into residue-residue interaction pairs employing the MM-GBSA decomposition method of the MMPBSA.py module of AMBER14 (Miller et al., 2012).



ลิขสิทธิ์มหาวิทยาลัยเชียงใหม่
Copyright© by Chiang Mai University
All rights reserved